International Journal of Nanomedicine

Dovepress
open access to scientific and medical research

Open Access Full Text Article

ORIGINAL RESEARCH

Antifungal effects of indolicidin-conjugated gold nanoparticles against fluconazole-resistant strains of *Candida albicans* isolated from patients with burn infection

This article was published in the following Dove Press journal:
International Journal of Nanomedicine

Hossein Rahimi[1]
Shahla Roudbarmohammadi[1]
Hamid Delavari H[2]
Maryam Roudbary[3]

[1]Department of Medical Mycology, Faculty of Medical Sciences, Tarbiat Modares University, Tehran, Iran; [2]Department of Materials Engineering, Faculty of Engineering, Tarbiat Modares University, Tehran, Iran; [3]Department of Medical Mycology and Parasitology, School of Medicine, Iran University of Medical Sciences, Tehran, Iran

Background: *Candida albicans* as an opportunistic fungus is one of the most important causes of late-onset morbidity and mortality in patients with major burns and severely impaired immune system. In recent years, the emergence of resistance to opportunistic fungi and toxicity of antimicrobial drugs make it necessary to develop new drugs.

Methods: In the present study, we investigated anticandidal effects of indolicidin, as a representative of host defense peptide, conjugated with gold nanoparticles in fluconazole-resistant clinical isolates of *C. albicans*. After characterizing the conjugation of indolicidin using biophysical methodologies, the cytotoxicity and hemolytic activity of the nanocomplex were examined. In addition, the expression level of *ERG11*, responsible for antifungal resistance, and the immunomodulatory effect of peptide-nanomaterial conjugates were assessed.

Results: Our data indicated that the nanocomplex was nontoxic for the fibroblast cells and erythrocytes. Treatment with the nanocomplex significantly reduced the expression levels of the *ERG11* gene in fluconazole-resistant *C. albicans* isolates and the *iNOS* gene in macrophages.

Conclusion: The study data provides a chance to develop innovative therapies for the treatment of *C. albicans* burn infections. However, further investigation is required to examine the efficiency of the nanocomplex.

Keywords: burn infection, *Candida albicans*, indolicidin, gold nanoparticles, antimicrobial peptides

Introduction

Burn injuries are among the most-destructive types of all injuries and a serious crisis in the medical profession and global public health, which can affect everyone in every aspect of the physical and mental environment.[1] Wounds are supportive environment for the growth of various microbial species, including fungi. The incidence of fungal infection, as reported in different documents, is from 6.3% to 44% according to various burn centers throughout the world.[2] One of the prevalent fungal infections in burn injuries is candidiasis and *Candida* spp. have historically been the most common invasive mycosis which can induce local or systemic infection. The incidence of invasive candidiasis burns cases varies widely, but it includes 3–23% of these infections with a mortality rate of between 14% and 74%.[3,4]

Traditional antifungal drugs including azoles, echinocandins, inhibitors of calcineurin, and Hsp90 are the most common therapies for candidiasis.[5] Fluconazole is

Correspondence: Shahla Roudbarmohammadi
Department of Medical Mycology, Tarbiat Modares University, POB 14155-4838, Tehran, Iran
Tel +98 218 288 4540
Fax +98 218 801 3030
Email sh.mohammadi@modares.ac.ir; shahla-Roudbarmohammadi@yahoo.com

submit your manuscript | www.dovepress.com
DovePress
http://doi.org/10.2147/IJN.S207527

most widely used to treat candidiasis infections due to its high bioavailability and low toxicity.[6] However, undirected clinical use of fluconazole and long-term exposure to the drug have led to the emergence of drug-resistant strains of *C. albicans*.[7] So it is imperative to discover new antifungal therapeutics as alternatives to conventional drugs to cope with drug resistance and eliminate the fungal infection in burn-injured individuals. Ideally, compared to traditional antibiotics, new drugs have multiple mechanisms of action and lower susceptibility to the development of resistance.[8]

Host defense peptides (HDPs) have been shown to increase the immune response against pathogenic organisms such as bacteria, fungi, parasites, and viruses.[9,10] Indolicidin is a cationic peptide enriched with tryptophan and proline residues that has been shown to have antimicrobial and antifungal properties with a low toxicity profile in vitro and in vivo.[11–13] Indolicidin proves a good candidate for therapeutic applications because of its broad spectrum of activity, its small size, naturally occurring, unique composition, and potentially different secondary structure.[14] It has been shown that indolicidin has a tendency to readily permeabilize the lipid bilayer of different compositions, but is distinct from other amphiphilic peptides in that the membrane permeabilization does not lead to lysis. Thus, it is demonstrated that indolicidin uses its membrane affinity property for entering the cytoplasm to exert its antimicrobial activity by preferential inhibition of DNA synthesis.[15,16] However, potential toxicity, high costs of production and instability to proteases limit the use of the peptides in clinics.[17,18] In this context, several studies have been conducted to overcome these limitations by functionalizing nanoparticles (NPs) with the peptides to improve their antimicrobial activity in vitro and in vivo.[19,20] It is widely accepted that multivalence may give greater efficiency and conjugation on NPs may reduce proteases degradation.[21]

Today, NPs are widely used in medicine against bacterial and fungal infections and have a low probability for resistance development by the pathogens. NPs consider suitable candidates for transporting drugs to their targets.[22,23] The combination of NPs with antimicrobial peptides makes it possible to decrease the cytotoxicity from both agents because of the synergistically enhanced antimicrobial activities and the reduced requirement for high dosages.[24,25] Gold NPs are considered to be comparatively safer than other inorganic NPs because of the inert and nontoxic nature of Au.[26] Additionally, the redox nature of Au is beneficial in reducing the level of reactive oxygen species produced during exposure to NPs.[25,26] The colloidal gold NPs have been used for therapeutic purposes for centuries that indicates the high biocompatibility of gold.[27–29] Several recent studies confirmed that gold NPs exhibit strong antimicrobial activity against the various clinical strains of the fungus *Candida*.[30–32]

Therefore, we hypothesized that by conjugating indolicidin with gold NPs, it would be possible to enhance the antimicrobial effects of indolicidin and reduce the cytotoxicity of both agents against fluconazole-resistant isolates of *C. albicans* in burn injuries. Here, we present a simple, two-step method for conjugation of indolidicin with gold NPs via chemisorption of thiols onto the spheres of the colloidal gold. Our results demonstrated that indolicidin-gold NPs conjugates showed higher antifungal activity and a lower cytotoxicity in comparison to free indolicidin and bare gold NPs. In addition, quantitative real-time PCR results indicated that the conjugates reduced the inducible NO synthase (*iNOS*) mRNA expression in *Candida*-stimulated macrophages, which showed the anti-inflammatory and immunomodulatory effects of the nanocomplex. Thus, we can conclude that indolicidin-gold NPs conjugates can act as effective antimicrobial agents.

Materials and methods

Materials and buffer solutions

Indolicidin was purchased from Santa Cruz Biotechnology, Inc. (Dallas, TX, USA), Hydrogen tetrachloroaurate ($HAuCL_4$), dimethyl sulfoxide (DMSO), 2-mercaptoethanol, PBS, sodium citrate dihydrate, Millipore-Q water, cyanogen bromide, acetonitrile, Sabouraud dextrose broth (SDB), Sabouraud dextrose agar (SDA), RPMI1640, MTT, Triton X-100, Brewer thioglycollate medium, Fluconazole, Trizol™ reagent were obtained from Thermo Fisher Scientific (Waltham, MA, USA).

Preparation and characterization of gold nanoparticles colloidal suspension

A stable suspension of monodisperse gold NPs with a diameter of about 30 nm was prepared according to standard procedure. In brief, a 1 mM aqueous solution of $HAuCl_4$ was prepared by dissolving 0.39 g of $HAuCl_4 \cdot 3H_2O$ in 1 L of Millipore-Q water, and a 38 mM solution of sodium citrate dehydrate by dissolving 11.41 g in 1 L of Millipore-Q water. An amount of 30 mL of the $HAuCl_4$ solution was put in a 50 mL beaker equipped with a magnetic bar. The solution was heated to the boiling point and then 3 mL of the citrate solution was added (Au:citrate molar ratio 1:3.8) under stirring. After about 2 mins, a deep wine-red sol was obtained. No further color change after prolonged boiling was

observed. General morphology of the synthesized AuNPs was characterized by transmission electron microscopy (TEM) (Carl Zeiss-EM10C-100 KV, Jena, Germany). The absorption property was determined by UV/Vis spectrometry (UV-1750; Shimadzu, Kyoto, Japan). The surface groups were detected by Fourier Transform Infrared Spectroscopy (FTIR) in a Perkin Elmer Instrument Spectrum GX spectrometer (PerkinElmer, Waltham, MA, USA). Zeta potential (ZP) measurements of gold NPs and indolicidin-gold NPs conjugates were performed using a Malvern Nanosizer Nano ZS (Malvern Instruments, Worcestershire, UK) at 25°C, pH 6 on the same condition of conjugation.

Synthesis and characterization of indolicidin-gold NPs conjugates

HDP, indolicidin, is a natural linear cationic cathelicidin containing five tryptophan and two proline residues (ILPWKWPWWPWRR-NH_2) with hydrophobic characteristics. The peptide was conjugated to the gold NPs using a simple, two-step method by the chemisorption of thiols onto the spheres of the colloidal gold; 5 mg of indolicidin was suspended in 25 µL of DMSO. The resulting solution was mixed properly followed by further addition of 975 µL of PBS to make a 5 mg/mL peptide solution. This solution was used as the stock peptide solution for our experiments; 100 µL of the 2-mercaptoethanol was added to 900 µL of the gold NPs solution. The solution was subsequently sonicated in an ultrasonic bath (VWR Ultrasonic Cleaner USC-TH, 45 kHz, 180 W) using a glass beaker for 30 mins and then incubated for 12 hrs at room temperature under slow vortex. Excess thiols were removed by twice centrifugation for 10 mins (at 15,700 g, 10°C), followed by decantation of supernatants. The purified thiol-stabilized gold NPs were redissolved in Millipore-Q water. The solution was adjusted to pH 10–11 by sodium carbonate/sodium hydrogen phosphate (0.001 M:0.05 M) buffer. After adding 3 µL of the cyanogen bromide (28 mM) and 40 µL of the stock 5 mg/mL peptide solution, the resulting solution was mixed thoroughly and stirred in the dark overnight at room temperature. Free peptides were removed from the conjugate mixture using molecular weight cut-off spin column (3 MWCO, Millipore, Billerica, MA, USA). Figure 1 depicts the basic algorithm of the synthesis scheme.

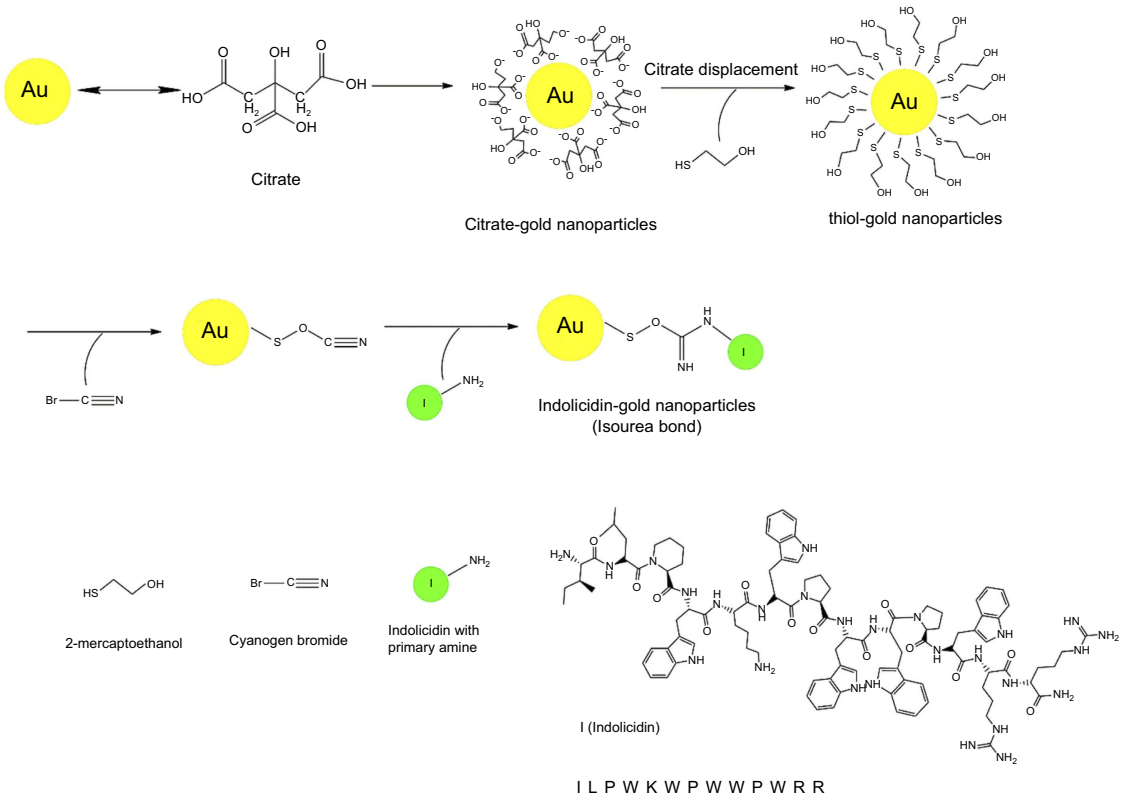

Figure 1 A schematic diagram of synthesis protocol of gold nanoparticles conjugation with indolicidin is shown. For conjugation of indolicidin with gold nanoparticles, thiol-stabilized gold nanoparticles were synthesized by adding 2-mercaptoethanol to provide hydroxyl groups. Then, cyanogen bromide used to activate hydroxyl groups on gold nanoparticles to create reactive cyanogen esters, which then attached to the primary amine of indolicidin by an isourea bond.

Preparation of *Candida albicans* isolates and culture condition

Ten clinical isolates of *C. albicans* were obtained from skin lesions of patients suffering from fungal infection that hospitalized at the Shahid Motahari burn center of Tehran. Moreover, *C. albicans* 10231, from ATCC (Manassas, VA, USA) was used as a reference strain in this study. The isolates had been taken as part of routine hospital laboratory procedures. The clinical strains were named C1-C10 and the reference strain was named CR. All isolates were cultured on SDA medium (1% peptone, 4% glucose, 1/5% agar, pH 5/6), incubated for 48 hrs at 37°C. Then, one colony of each isolate was immersed to 10 mL of SDB. After 24 hrs incubation at 37°C, *Candida* cells were harvested by centrifugation (1500 rpm, 10 mins), washed with PBS, and 10 mL of RPMI1640 medium was added to each to 10^5 cells/mL.

Determination of minimum inhibitory concentration (MIC) and minimum fungicidal concentration (MFC)

The antifungal effects of gold NPs, indolicidin, and indolicidin-gold NPs conjugate on all *Candida* isolates were determined by the broth micro-dilution susceptibility assay based on the Clinical and Laboratory Standard Institute (CLSI).[33] Free indolicidin with initial concentration (200 µg/mL) diluted with RPMI medium, both conjugated indolicidin and bare gold NPs diluted with Millipore-Q water. Each diluted component was added to 100 µL of *Candida* suspension separately for further evaluation. Free indolicidin and conjugated indolicidin were tested at concentrations ranging from 0.78 to 200 µg/mL. Bare gold NPs were tested at the concentrations ranging from 3.04 to 390 µg/mL. Fluconazole (Sigma-Aldrich, St Louis, MO, USA) at concentrations ranging from 0.5 to 256 µg/mL served as the standard antifungal drug. Species-specific breakpoints were approved from CLSI-M27/S4.[34] MIC was read visually after 24 hrs and noted as the lowest concentration of fluconazole, gold NPs, indolicidin, and indolicidin-gold NPs conjugates resulting in at least 50% reduction of growth compared to the control. The MIC breakpoints for fluconazole were determined as susceptible (MIC ≤2 µg/mL), and resistant (MIC ≥64 µg/mL). The MFC was determined by subculturing 10 µL of the medium collected from the wells showing no microscopic growth after 48 hrs, on SDA medium plates. The MFC was the lowest concentration that yielded no colonies after 24 hrs plates incubation. The MFC/MIC ratio was calculated to determine whether the substance had fungistatic (MFC/MIC ≥4) or fungicidal (MFC/MIC <4) activity.

Isolation and culture of murine peritoneal macrophages

Six- to eight-week-old BALB/c mice were purchased from the Pasteur Institute (Tehran, Iran). All animals were kept under standard condition in the animal house at Tarbiat Modares University until the completion of experiment; 1 mL of 3% Brewer thioglycollate medium was injected into the peritoneal cavity of each mouse. After 4–5 days, at first, all mice were anesthetized with xylazine/ketamine, then euthanized by rapid cervical dislocation; 5 mL of ice-cold PBS (with 3% FBS) was injected into the peritoneal cavity. After performing a gentle massage on the peritoneal cavity, the fluid carefully aspirated and collected in tubes on ice. The peritoneal cells were resuspended in RPMI medium 1640 after centrifuging for 10 mins at 400 g. The cell concentration was adjusted to 1.5×10^6 cells/mL in RPMI medium. The cells were allowed to adhere into the 6-well plates by culturing them for 2 hrs at 37°C and non-adherent cells were removed by gently washing 3 times with warm PBS. All animal experiments and procedures were carried out according to the ethical standards and protocols approved by the Committee of Animal Experimentation of Tarbiat Modares University, Tehran, Iran (IR. TMU. REC. 1395. 351).

Total RNA extraction and quantitative RT-PCR analysis

A suspension containing 1×10^6 cells/mL of *C. albicans* ATCC 1023 (fluconazole-sensitive strain) and *C. albicans* isolates (fluconazole-resistant isolates) were treated with fluconazole (64 µg/mL), bare gold NPs (24.37 µg/mL), free indolicidin or indolicidin-gold NPs conjugates (12.5 µg/mL). All isolates were treated with a same dose of free indolicidin or indolicidin-conjugated gold NPs (12.5 µg/mL) for relative comparison analysis. Total RNA was extracted from *Candida* isolates (treated or non-treated) using the Trizol™ reagent (Thermo Scientific, Waltham, MA, USA) and glass beads (0.45 mm diameter). Total RNA was also extracted from each treated or non-treated macrophage cells using the RNeasy mini kit (Qiagen, Valencia, CA, USA). The quality and amount of purified RNA were analyzed with a Nanodrop™ 2000 spectrophotometer (Thermo Scientific). Briefly, 1,000 ng of RNA was reverse transcribed with the first strand cDNA synthesis

kit (Fermentase, Germany). Real-time PCR was carried out using AMPLIQON master mix (Real Q plus 2, master mixes green high ROX, Sinnacolon Co., Tehran, Iran) in StepOnePlus real-time PCR detection system (Applied Biosystems; Thermo Scientific, Waltham, MA, USA) by using a sybergreen master mix. The primers used in this study are listed in Table 1. All experiments were independently performed in triplicate, and data from real-time PCR analyses were determined by the Applied Biosystems™ StepOne software. Calculation of relative gene expression was performed using the comparative critical threshold ($\Delta\Delta C_T$) method in which the amount of the target genes was adjusted to the reference gene (*ACT1* or *GAPDH* gene).

Hemolytic activity

Five mL of blood was collected from healthy volunteers and centrifuged at 1,000 rpm for 10 mins at 4ºC. Plasma was removed carefully and the erythrocytes were then washed for additional three times with PBS, pH 7.4 for 5 mins; 90 µL of diluted erythrocytes (100 µL erythrocytes suspension plus 900 µL PBS) was mixed with 10 µL of bare gold NPs, free indolicidin, conjugated indolicidin, fluconazole, 10 µL of PBS as a negative control, or 10 µL of Triton X-100 as a positive control. The reaction mixture was incubated at 37ºC water bath for 60 mins. The volume of reaction mixture was reached to 1 mL by adding 900 µL of PBS. Finally, it was centrifuged at 300 rpm for 5 mins and the resulting hemoglobin in the supernatant was measured at 540 nm by spectrophotometer to determine the concentration of hemoglobin. The percentage of hemolysis was calculated as follows:

$$\text{Hemolysis inhibition}(\%) = [(\text{Abs in the sample} - \text{Abs in PBS}) / (\text{Abs in 0.1\% Triton X-100} - \text{Abs in PBS})] \times 100$$

Cell viability assay

The cytotoxic effects of indolicidin-gold NPs conjugate on the viability of the NIH3T3 cell line evaluated using MTT assay.[35,36] The NIH3T3 fibroblast cell line was obtained from ATCC, grown in DMEM medium supplemented with 10% FBS and 1% pen/strep and then seeded at a density of 0.2×10^6 cells/well onto 6-well plate. After overnight plating, cells were treated with fluconazole (64 µg/mL), bare gold NPs (24.37 µg/mL), free indolicidin or indolicidin-gold NPs conjugates (12.5 µg/mL) for 48 hrs. After this time, 20 µL of MTT (5 mg/mL in PBS) was added to each well and the plates were incubated for 4 hrs. Then, the supernatants were gently removed and the formazan crystals generated with MTT reduction by the living cells were extracted by the addition of 100 µL DMSO. The plates were incubated for 30 mins at 37ºC and the OD was read at 550 nm, with a reference at 655 nm in a microplate reader. Viability was calculated as the ratio of the mean of OD obtained for each condition to that of control condition (negative control).

Statistical analysis

All tests were carried out three times, and the results were shown as mean ± SD. One-way ANOVA test was used to determine significant differences between groups by SPSS software (version 16.0 for windows; SPSS Inc., Chicago, IL, USA), and *P*-value <0.05 was considered statistically significant.

Table 1 Detailed information about the primers used in this study

Genes	Sequences	Fragment size (bp)	Tm (°C)
ERG11	F 5′-TTTGGTGGTGGTAGACATA-3′	134	58
	R 5′-GAACTATAATCAGGGTCAGG-3′		
ACT1	F 5′-CCAGCTTTCTACGTTTCC-3′	209	60
	R 5′-CTGTAACCACGTTCAGAC-3′		
iNOS	F 5′-ACAACAAATTCAGGTACGCTGTG-3′	84	60
	R 5′-TCTGATCAATGTCATGAGCAAAGG-3′		
GAPDH	F 5′-TGCACCACCAACTGCTTAGC-3′	87	60
	R 5′-GGCATGGACTGTGGTCATGAG-3′		

Abbreviations: F, forward primer; R, reverse primer; Tm, melting temperature.

Results

Characterization of gold NPs and indolicidin-gold NPs conjugates

UV-vis spectrum, TEM image, and DLS graph are shown in Figure 1A–C, respectively. From the data of the UV-vis absorption spectrum shown in Figure 2A, it was found that gold NPs have a peak of absorbance at a wavelength of 521 nm (curve i). After adding the 2-mercaptoethanol to the gold NPs, the intensity of the transverse band decreased, and a red-shifted plasmon band at 640 nm was obtained (curve ii). The color changes from deep red to light blue, indicating the formation of assembly of gold NPs. Then, the mixture was sonicated for 60 mins to disperse the thiol-stabilized gold NPs. Pulses with a 50% amplitude and a sequence of 2 s on and 2 s off were used during the sonication process. The color of the solution changed from blue to light red after ultrasonication, and a surface plasmon resonance band at 521 was obtained, indicating the dispersion and remove the aggregation of the NPs (curve iii). The peak at 390 nm which is shown in curve (iv) appeared after adding indolicidin to the thiol-stabilized NPs, indicating the conjugation of the peptide to the gold NPs. Figure 2B confirms the shape of gold NPs in colloidal solution. It is obvious that gold NPs are mainly spherical, uniform in size and the average size is 30 nm. Based on Figure 2C(1), the size distribution of colloidal gold NPs was near 30 nm, and the average size of particles was approximately 32 nm. Moreover, the finding revealed that the ZP of gold NPs is −29.3 mV (Figure 2C(2)).

In addition, ZP (mV) of conjugated and non-conjugated forms was measured and presented in Figure 2C(2)–C(4). The ZP of thiol-gold NPs was −17.4 mV (Figure 2C(3)), while one of the gold NPs was −29.3 mV. Gold NPs have a higher negative charge in comparison with thiol-gold NPs. Besides, the ZP of gold NPs conjugated with indolicidin was −4.7 mV while that of thiol-gold NPs was −17.4 mV as shown in Figure 2C(4). It is notable that gold NPs conjugated with the peptide have a lower negative charge in comparison to thiol-gold NPs. Moreover, the size distribution of the thiol-gold NPs and indolicidin-conjugated gold NPs were near 40 and 139 nm, respectively (Figure S1). Therefore, these results indicate successful binding of the peptides molecules to the surface of gold NPs.

Figure 3 shows the FTIR spectroscopy results for the individual indolicidin and their nanostructures with gold NPs or thiol-stabilized gold NPs. The prominent stretching band was found at around 2,950 cm^{-1} in thiolated gold NPs, whereas this band was not present in gold NPs, indicating mercaptoethanol binds with the surface of gold NPs through the formation of an Au–S bond. In addition, FTIR spectroscopy confirmed that indolicidin is covalently conjugated with gold NPs. There were the characteristic stretching peaks at 1,650 and 985 cm^{-1} in free indolicidin and gold NPs-Indolicidin conjugate, whereas these peaks were not found in gold NPs and thiolated gold NPs. The split peaks at around 1,100 and 985 cm^{-1} represent C–N stretch in an isourea bond. The characteristic spectra of the bare gold NPs and free peptide dispersions were compared to those of the conjugates where the conjugates showed remarkable band shifts and occurrence of newer bands indicating a successful conjugation reaction.

The results of antifungal susceptibility test

The MIC and MFC of indolicidin, gold NPs and conjugated indolicidin against 10 isolates of *C. albicans* are presented in Table 2. As shown, the MIC of conjugated indolicidin was less than the MIC of free indolicidin ($P<0.05$). Furthermore, the MFC of conjugated indolicidin was less than the free indolicidin ($P<0.05$). The MIC of indolicidin attached to the gold NPs was less than the MIC of fluconazole as a chemical drug. The MIC for 8 clinical isolates was 64 μg/mL for fluconazole, but two isolates were highly resistant, with MIC ≥64 μg/mL. Nevertheless, all isolates were susceptible to the conjugated indolicidin, with MIC ≤12.5 μg/mL, while the MFC was two times higher than the MIC for 80% of the isolates. The MIC of gold NPs for the growth inhibition of *C. albicans* isolates was 24.37 μg/mL. The gold NPs at a concentration of 2.437 μg/mL, when capped with 12.5 μg/mL of indolicidin, inhibited the growth of *C. albicans* significantly. Addition of gold NPs caused a significant decrease in the MIC of indolicidin, ie, MIC decreased from 50 to 12.5 μg/mL. Moreover, the MIC of fluconazole for *C. albicans* 10231 was 2 μg/mL. The comparative analysis of MIC and MFC indicated that MFC of fluconazole was two times higher than MIC for 8 (80%) *C. albicans* isolates. The MFC of conjugated indolicidin was two times higher than the MIC for 8 (80%) *C. albicans* isolates, while 20% of the isolates had the same values of MIC and MFC of conjugated indolicidin.

Cytotoxicity studies of indolicidin-gold NPs conjugates using MTT assay

To assess the cytotoxic effect of the various components, we determined the viability of NIH3T3 fibroblast cell line.

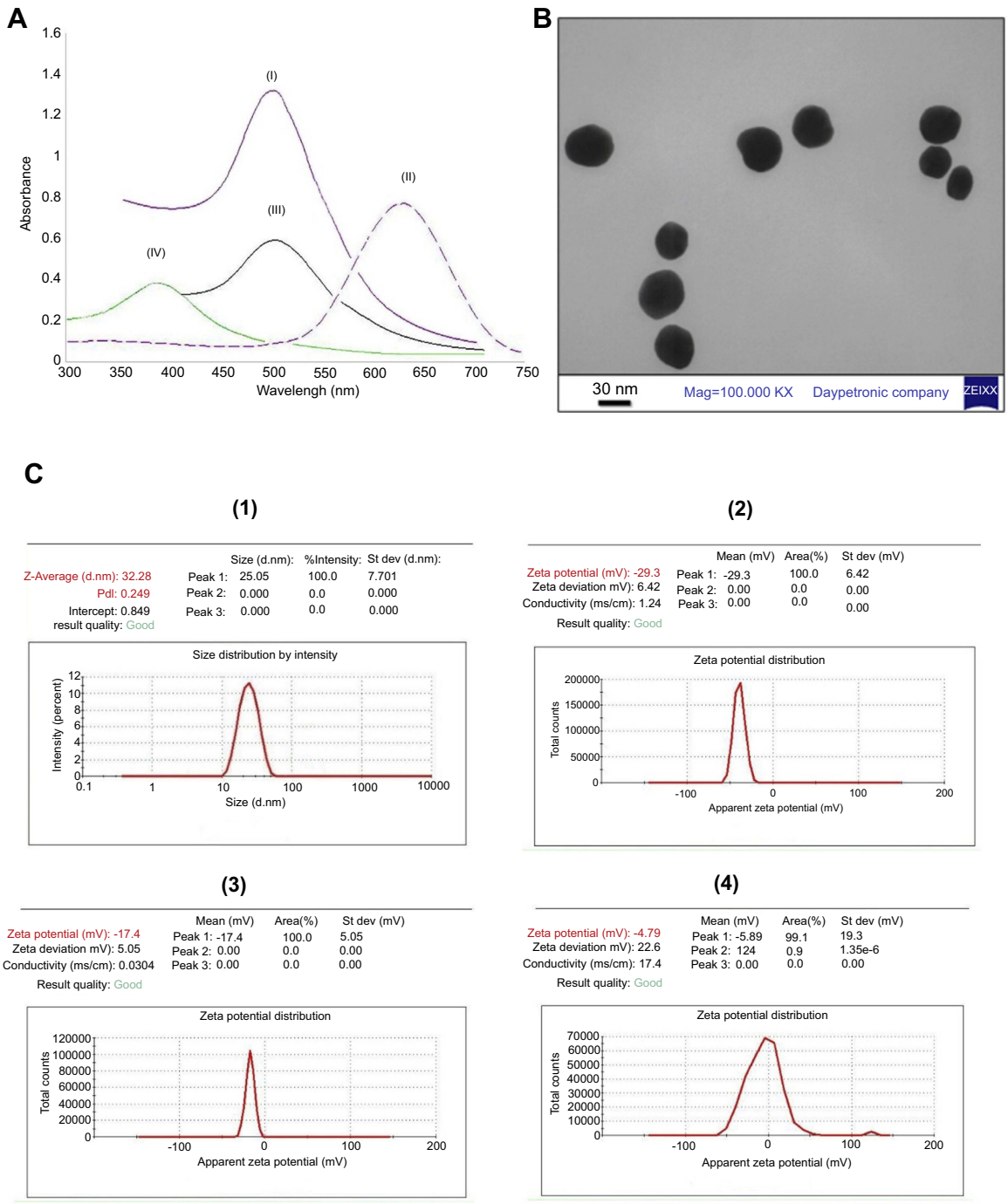

Figure 2 Characterization of gold NPs and indolicidin-gold NPs conjugate. (**A**) UV-vis spectrum of gold NPs (I), thiol-capped gold NPs before sonication (II), thiol-capped gold NPs after sonication (III) and the gold NPs conjugated with indolicidin (IV). (**B**) The TEM image of colloidal gold NPs. (**C**) DLS graph of colloidal gold NPs with an average diameter of 32 nm (1) and the zeta potential of gold NPs (2), thiol-capped gold NPs (3) and indolicidin conjugated with gold NPs (4).
Abbreviations: NPs, nanoparticles; TEM, transmission electron microscopy; DLS, Dynamic light scattering.

Viability curves were obtained for free indolicidin and conjugated indolicidn for a given concentration range. Figure 4A shows the dose–response curves on NIH3T3 viability obtained for the unconjugated and the conjugated form of indolicidin. Indolicidin-conjugated gold NPs were found significantly less toxic than the free indolicidin, with the calculated IC_{50} of 57.59 and 24.35 µg/mL, respectively ($P<0.05$). Moreover, the dose–response curves were obtained for gold NPs and fluconazole for a given range of concentrations (Figure 4B and C). Following 48 hrs

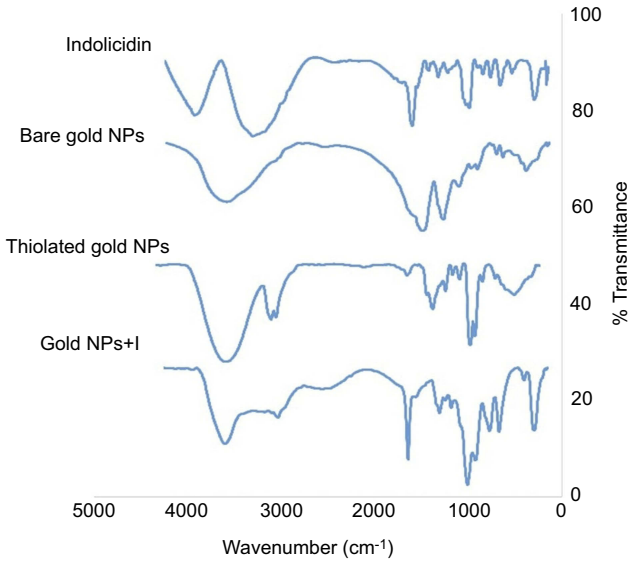

Figure 3 FTIR spectra. Representative fourier transformed infrared spectra of free indolicidin, bare gold NPs, thiol-capped gold NPs and indolicidin conjugated with gold NPs (gold NPs-I) are shown.
Abbreviations: FTIR, fourier-transform-infrared spectroscopy; I, indolicidin; NPs, nanoparticles; gold NPs-I, indolicidin-gold nanoparticles conjugates.

exposure time, the IC_{50} of fluconazole was 73.65 µg/mL and the gold NPs exhibited the IC_{50} as 118.35 µg/mL. These results suggested that the conjugated indolicidin with gold NPs was more biocompatible than free indolicidin. Furthermore, when the gold NPs were functionalized with indolicidin as complex, cytotoxicity was greatly decreased.

Expression analysis of ERG11 gene in *C. albicans* isolates

Effect of the different components on *ERG11* gene expression of *C. albicans* isolates in comparison to *C. albicans* ATCC 10231 as susceptible control stain was evaluated by real-time PCR assay (Figure 5). In comparison to the control strain, the overexpression of *ERG11* in all isolates (which treated with 64 µg/mL of fluconazole) was observed ($P<0.05$). In contrast, the *ERG11* expression was reduced about 1–2 fold in the isolates treated with 12.5 µg/mL of free indolicidin and about 2–3 fold in the isolates treated with 12.5 µg/mL of conjugated indolicidin in comparison to the untreated control group ($P<0.05$). The *C. albicans* ATCC 10231 was also capable of down-regulating *ERG11* in response to free or conjugated indolicidin exposure ($P<0.05$). In addition, the real-time PCR analyses revealed the down-regulation of the *ERG11* gene in all *C. albicans* isolates exposed to bare gold NPs with a concentration of 24.37 µg/mL ($P<0.05$). The obtained results demonstrated that the fluconazole-resistant *C. albicans* isolates were susceptible to indolicidin-gold NPs conjugates.

Table 2 The MIC and MFC of free indolicidin, bare gold nanoparticles, and indolicidin-gold nanoparticles conjugate against 10 isolates of *Candida albicans*. MIC was determined as the lowest concentration resulting in at least 50% reduction of growth compared to the control

	MIC (µg/mL)	MFC (µg/mL)	MFC/MIC ratio
Free indolicidin	50	150	3 fungicidal
Gold nanoparticles	24.37	97.5	4 fungistatic
Conjugated indolicidin	12.5	25	2 fungicidal

Abbreviations: MIC, minimum inhibitory concentration; MFC, minimum fungicidal concentration.

Evaluation of hemolytic activity of indolicidin-gold NPs conjugates using mammalian erythrocytes

Hemolytic activity of gold NPs, free indolicidin, and conjugated indolicidin was evaluated using human erythrocytes. Free indolicidin at concentrations ranging from 0.78 to 50 µg/mL caused little hemolysis effect (in the range of 1–20%) whereas at higher concentrations ranging from 100 to 200 µg/mL significant hemolysis was detected. In contrast, indolicidin-conjugated gold NPs showed non-significant hemolysis at concentrations ranging from 0.78 to 100 µg/mL and significant hemolysis at higher concentrations (Figure 6A). Also, gold NPs concentrations ranging from 3.04 to 97.5 µg/mL did not cause significant hemolysis, and >90% of human erythrocyte did not show hemolysis. Gold NPs at concentrations ranging from 195 to 390 µg/mL caused significant hemolysis (Figure 6B). Moreover, fluconazole hemolytic activity showed that at a concentration of 1–32 µg/mL, there was little hemolysis, but in higher concentrations, it caused significant hemolysis in human erythrocytes (Figure 6C). So, these results indicate that indolicidin in both conjugated or non-conjugated forms has less hemolytic activity compared to fluconazole. Moreover, indolicidin-gold NPs conjugates showed lower hemolysis in comparison to free indolicidin.

Effect of conjugated or non-conjugated indolicidin on iNOS gene expression in macrophages

To examine the immunomodulatory effects of indolicidin peptide, we assessed the nitric oxide (NO) production

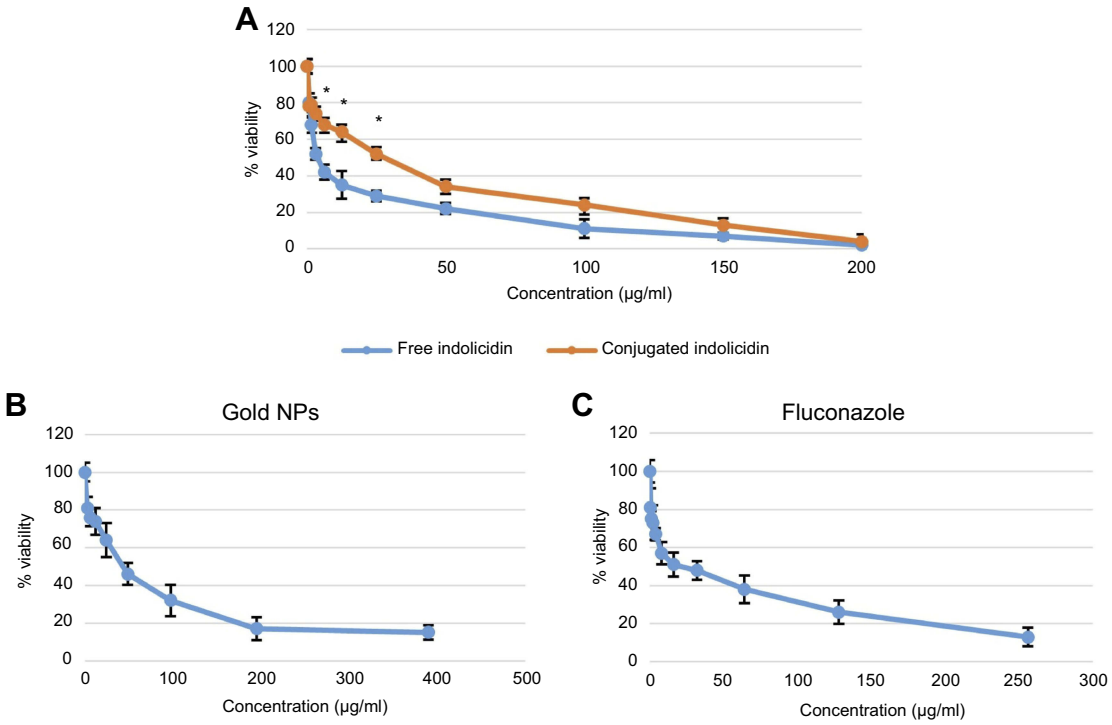

Figure 4 Evaluation cytotoxicity effects of the bare gold NPs, indolicidin-gold NPs, free indolicidin and fluconazole on NIH3T3 cell line after 48 hrs treatments. Dose-dependent effects of free indolicidin in comparison to the indolicidin-gold NPs conjugates in different concentrations (**A**), bare gold NPs (**B**) and fluconazole (**C**) on the viability of NIH3T3 cells are shown. Each data point represents the mean±SD of three replicates.
Abbreviation: NPs, nanoparticles.

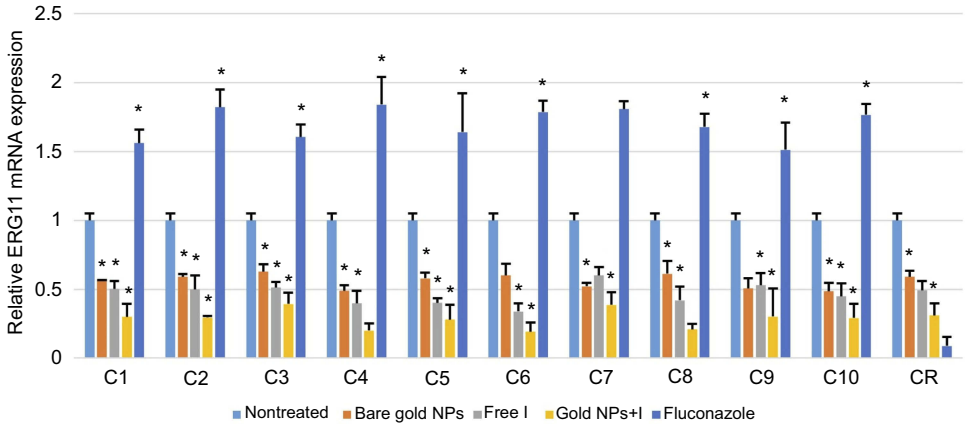

Figure 5 Expression analysis of the *ERG11* gene in *Candida albicans* isolates exposed to the bare gold NPs, indolicidin-gold NPs, free indolicidin, and fluconazole after 24 hrs of cultivation. The relative expression of the *14α-demethylase* (*ERG11*) gene relative to that of the internal control *ACT1* gene in 10 *C. albicans* isolates obtained from the burn patients suffering from candidiasis and the control strain ATCC 1023 in comparison to the non-treated group is shown. The data are presented as mean±SD, calculated from three independent experiments (*P<0.05).
Abbreviations: NPs, nanoparticles; gold NPs-I, indolicidin-gold nanoparticles conjugates; C1-C10, *C. albicans* strains isolated from burn patients suffering from candidiasis; CR, *C. albicans* ATCC strain 1023.

indirectly by the mice peritoneal macrophages following conjugated or non-conjugated indolicidin treatment by the changes in nitric oxide synthase (*iNOS*) gene expression levels. NO production by macrophages plays a dual role; NO can rapidly convert to a reactive oxygen species with potent antimicrobial activity, whereas sustained high levels may lead

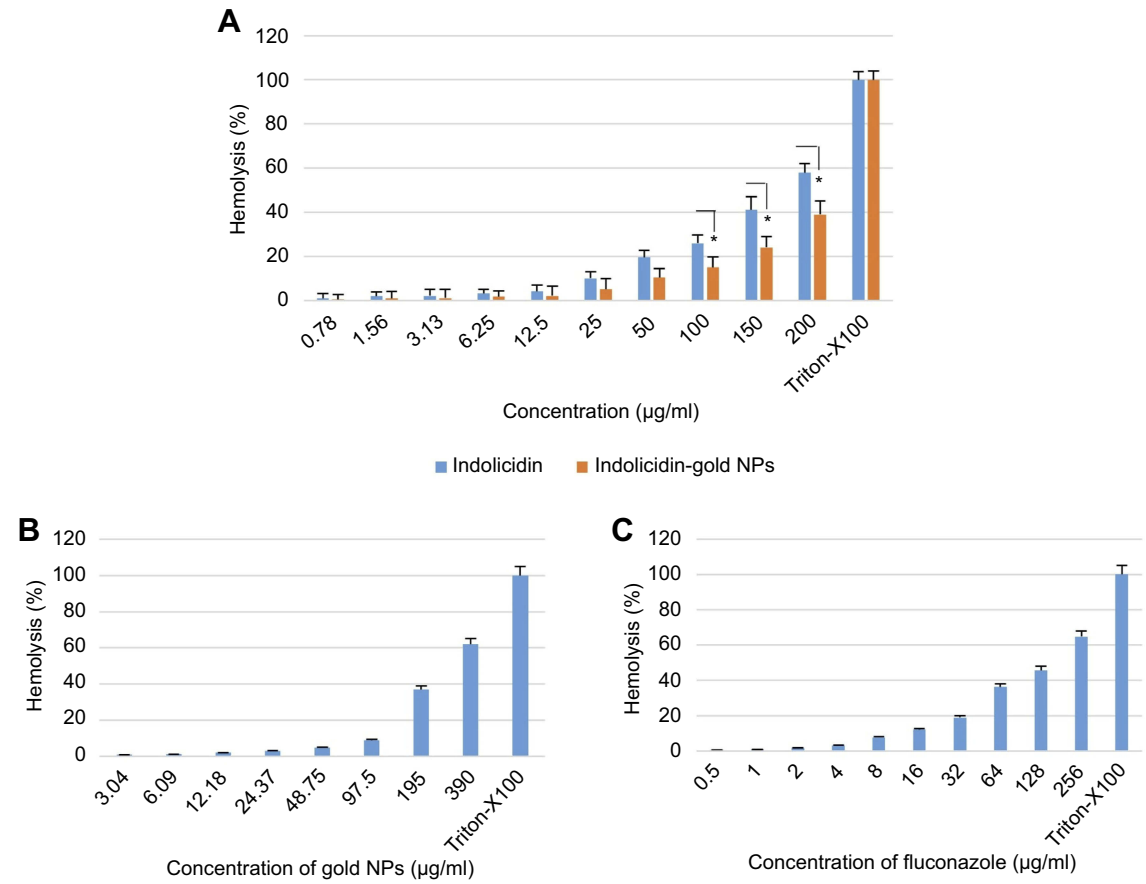

Figure 6 Evaluation of the hemolytic activity. The hemolytic activity of free indolicidin, conjugated indolicidin, bare gold NPs, and fluconazole were determined using human erythrocytes. Hemolytic activity of free indolicidin and indolicidin conjugated with gold NPs (**A**), bare gold NPs (**B**) and fluconazole (**C**) were measured in comparison with Triton X-100 treated erythrocytes as control cells. Data presented are the means of three independent experiments±SD.
Abbreviation: NPs, nanoparticles.

to tissue damage and cell death. Figure S2 shows the morphology of macrophages isolated from the mice peritoneal cavity after 2, 7, and 14 days of culture. As shown in Figure 7, *C. albicans* cells induced robust expression of *iNOS*, indicating that the macrophages are activated in response to fungal antigens. The expression level of *iNOS* mRNA was significantly reduced when the free indolicidin (as a cationic antifungal peptide) or conjugated indolicidin were incubated with macrophages in the presence of *C. albicans* ($P<0.05$). In contrast, the expression level of *iNOS* mRNA was slightly decreased following fluconazole or gold NPs treatments in the presence of *C. albicans*.

Discussion

Due to the increasing incidence of fungal infections in immunocompromised burn patients and the challenge of drug resistance, it is necessary to design the new antifungal components.[37] Because of their antimicrobial activities, the combination of antimicrobial peptides and metal NPs is a promising tool to combat drug-resistant pathogens.[22] Antimicrobial peptide-conjugated gold NPs are particularly attractive components due to the non-toxic nature of gold and the possibility of fine-tuning the peptide-NPs conjugation chemistry.[38,39] We reported here conjugation of indolicidin with the gold NPs using a simple, two-step chemisorption method to evaluate its synergistic antifungal effects on fluconazole-resistant *C. albicans* isolates.

In the first step, colloidal gold NPs were synthesized and characterized. The obtained result was similar to the previous studies showing an absorption peak at 521 nm on a size of 30 nm with a ZP of −29.3 mV.[40,41] It confirmed the formation of the negative charge of the surface of gold NPs. The negative charge resulted from citrate that is used both as a reducing and a stabilizing agent of gold NPs. To conjugation of indolicidin with gold NPs, thiol-stabilized gold NPs were synthesized by adding 2-mercaptoethanol, followed by functionalization of gold NPs using cyanogen bromide. The first step is the displacement of citrate by a

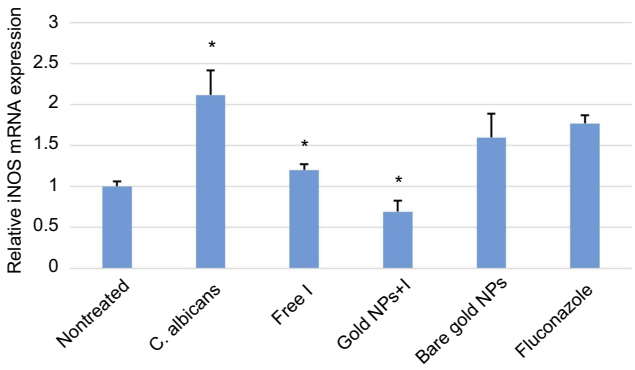

Figure 7 Quantitative RT-PCR analysis of the *iNOS* gene in murine macrophages incubated with the *Candida albicans* after 24 hrs treatment with bare gold NPs, free indolicidin, indolicidin conjugated with gold NPs, and fluconazole. The relative levels of gene expression are presented as fold changes in the treated groups with respect to the nontreated control. The gene transcript level was normalized against the *GAPDH* gene expression. Statistically significant differences between the *C. albicans*-treated group and the nontreated group, and between the *C. albicans*-treated group and the other treated groups (*P<0.05). The data shows mean±SD of three independent experiments.

Abbreviations: I, indolicidin; NPs, nanoparticles; gold NPs-I, indolicidin-gold nanoparticles conjugates.

relatively short thiol that exhibits strong interactions with gold and provides hydroxyl groups. Then, cyanogen bromide used to activate hydroxyl groups on gold NPs to create reactive cyanate esters, which then coupled to amine-containing peptides to form an isourea bond. Unlike the previous methods for activation of hydroxyls on particles, cyanogen bromide is used under aqueous condition, thus eliminating the need for organic solvents. After adding the surfactant (2-mercaptoethanol) to the gold NPs, another peak appeared at 640 nm, which suggests the change in color from red to light blue that indicates the formation of assembly or aggregated nanostructures. The absorbance peak at 640 nm disappeared and the absorbance peak at 521 nm reappeared upon applying the sonication which suggests the formation of dispersed thiol-capped gold NPs. Blueshift observed upon conjugation of indolicidin with gold NPs indicates a more hydrophobic environment of tryptophans present in indolicidin. Moreover, thiol-capped gold NPs had a lower negative charge in comparison to gold NPs, and gold NPs conjugated with indolicidin had a lower negative charge compared to thiol-capped gold NPs. FTIR results demonstrated that a few specific split peaks were formed as a result of the conjugation of indolicidin with gold NPs as compared to the indolicidin or gold NPs. Specific split peaks were observed at the fingerprint region (around 980–1,100 cm^{-1}) of the spectra signifying the formation of new bands for indolicidin-gold NPs conjugates. Therefore, it indicates the successful conjugation of indolicidin with gold NPs.

After synthesis and characterization of indolicidin-gold NPs conjugates, the antifungal activity of gold NPs, free indolicidin, indolicidin-gold NPs conjugates, and fluconazole against 10 clinical isolates of *C. albicans* was evaluated by the micro-dilution method. As demonstrated, the MIC of indolicidin-conjugated gold NPs was less than MIC of free indolicidin, bare gold NPs, and even fluconazole. Interestingly, the MFC data demonstrated that indolicidin-conjugated gold NPs and free indolicidin had fungicidal activity, whereas bare gold NPs had fungistatic activity. So, the indolicidin-gold NPs conjugates can be used as promising and novel antifungal agent to inhibit the growth of fluconazole-resistant *C. albicans*. It has been reported that conjugation of antimicrobial peptides with NPs resulted in enhance antimicrobial activity.[30,42] This could be due to the enhanced stability of the nanocomplex towards protease degradation and the enhanced drug efficacy by overcoming resistance mechanisms.[21,43,44]

In the next step, mRNA level of *ERG11*, which has been correlated with drug resistance in *C. albicans*, was evaluated following bare gold NPs, free indolicidin, indolicidin-gold NPs conjugates, and fluconazole treatments. Quantitative real-time PCR analysis demonstrated that *ERG11* mRNA was transcribed at a higher level in the all 10 clinical isolates of *C. albicans* (resistant isolates) than in the ATCC 10231 (susceptible strain) after 24 hrs treatment with fluconazole at the MIC concentration. Noticeably, down-regulated expression of the *ERG11* gene was found in *C. albicans* isolates treated with free indolicidin or indolicidin-gold NPs conjugates at the MIC concentrations. Moreover, the expression of *ERG11* gene reduced following gold NPs treatment. This indicates that gold NPs have considerable anti-fungal properties that could reduce the resistance of *C. albicans* isolates to the antimicrobial peptide by decreasing the expression of the drug resistance genes. It is noteworthy that the *ERG11* gene was less expressed in response to the nanoconjugated form of indolicidin compared to the free-form of indolicidin. These results demonstrated that fluconazole-resistant isolates of *C. albicans* were susceptible to indolicidin-gold NPs conjugates.

Host cytotoxicity of antimicrobial peptides and NPs is a major limitation in their application as antimicrobial agents. Therefore, we investigated the effect of indolicidin as nonconjugated or conjugated with gold NPs on NIH3T3 cells viability and hemolytic activity against human erythrocytes.[35,36] Cell viability findings represented that

free indolicidin had a more toxic effect on the growth of the eukaryotic cell, NIH3T3, compared to the indolicidin-conjugated gold NPs. In addition, cell viability assay showed that gold NPs at concentrations >150 µg/mL significantly reduced the viability of the cells. Furthermore, in the hemolytic assay, we observed minimal hemolysis with free or conjugated indolicidin, even at high concentrations, however, it was found that the conjugation of indolicidin to the gold NPs reduced the hemolysis of the erythrocytes compared to the free indolicidin. Surprisingly, the hemolysis experiment revealed that gold nanoparticles at concentrations >150 µg/mL and fluconazole at concentrations ≥64 µg/mL resulted in prominent erythrocytes hemolysis. Taken together, free indolicidin and indolicidin conjugated with gold NPs could not be toxic towards fibroblast cells and erythrocytes, which could overcome a challenge in their development as pharmaceutical drugs.

Finally, we evaluated the immunomodulatory and anti-inflammatory effects of indolicidin as a potent cationic antimicrobial peptide. Previous studies have shown that *C. albicans* infection resulted in increased expression of *iNOS* in macrophages.[45–48] NO is a marker of inflammation and is part of the non-specific host defense.[49] NO is synthesized by *iNOS* which is up-regulated during inflammatory condition such as fungal infections. However, overproduction of NO leads to a variety of diseases such as malignancy, rheumatoid arthritis, tissue injuries and septic shock.[50,51] Therefore, the down-regulation of NO is very important factor for the treatment of these conditions. We found that *iNOS* expression level significantly increased in peritoneal macrophages exposed to *C. albicans*. Our results indicated that the *iNOS* mRNA expression was significantly decreased by free indolicidin treatment in macrophages, but treatment with the indolicidin-gold NPs conjugates reduced the *iNOS* mRNA expression more significantly. In agreement with our findings, others have previously shown that many cationic antimicrobial peptides potently inhibit the expression of *iNOS* mRNA in macrophages. Also, our results proved that the *iNOS* mRNA expression level was also reduced after the gold NPs and fluconazole treatments in the macrophages exposed to *C. albicans*. This effect could be due to the reduction of fungi burden after the gold NPs and fluconazole treatments. However, the effect of gold NPs or fluconazole on reducing the *iNOS* mRNA expression level was less than that of the free indolicidin or indolicidin-gold NPs conjugates.

In conclusion, we used a two-step method for conjugating indolicidin peptides to gold NPs in order to assess the antifungal activity against candidiasis in burn patients. As presented by the various techniques and the physical characterization experiments, we could conjugate indolicidin to the gold NPs. The conjugates with the lower MIC against fluconazole-resistant *Candida* isolates and the lower cytotoxicity effects on eukaryote cells showed higher antimicrobial activity against the clinical isolates. Results from qRT-PCR experiments revealed that the clinical isolates of *C. albicans* were more susceptible to the indolicidin-gold NPs conjugates than free indolicidin or fluconazole. Moreover, our findings indicated that the nanocomplex significantly inhibited the expression of *iNOS* mRNA in macrophages and had a potent anti-inflammatory effect. The results presented in this research exhibited a preliminary study for the possible use of the indolicidin-gold NPs conjugates as a therapeutic alternative to combat fluconazole-resistant *Candida* isolates in burn patients, avoiding the adverse effects caused by the use of high doses of drugs. Further studies, especially involving animal models should be conducted to assess the indolicidin-gold NPs conjugates potential use as antifungal drugs in the systemic and topical applications.

Funding

This research is financially supported by Tarbiat Modares University.

Acknowledgment

The authors would like to thank Dr. Zahra Naseri for her helpful advice on various technical issues examined in this paper. We also thank Mrs. Karen Fascioli for editing the manuscript.

Disclosure

The authors report no conflicts of interest in this work.

References

1. Smolle C, Cambiaso-Daniel J, Forbes AA, et al. Recent trends in burn epidemiology worldwide: a systematic review. *Burns*. 2017;43(2):249–257. doi:10.1016/j.burns.2016.08.013
2. Murray CK, Loo FL, Hospenthal DR, et al. Incidence of systemic fungal infection and related mortality following severe burns. *Burns*. 2008;34(8):1108–1112. doi:10.1016/j.burns.2008.04.007
3. Eggimann P, Garbino J, Pittet D. Management of *Candida* species infections in critically ill patients. *Lancet Infect Dis*. 2003;3(12):772. doi:10.1016/S1473-3099(03)00831-4
4. Holzheimer R, Dralle H. Management of mycoses in surgical patients-review of the literature. *Eur J Med Res*. 2002;7(5):200–226.
5. Cowen LE. The evolution of fungal drug resistance: modulating the trajectory from genotype to phenotype. *Nat Rev Microbiol*. 2008;6(3):187. doi:10.1038/nrmicro1835

6. Sarkar S, Uppuluri P, Pierce CG, Lopez-Ribot JL. In vitro study of sequential fluconazole and caspofungin treatment against *Candida albicans* biofilms. *Antimicrob Agents Chemother*. 2014;58(2):1183–1186. doi:10.1128/AAC.01745-13
7. Youngsaye W, Hartland CL, Morgan BJ, et al. ML212: a small-molecule probe for investigating fluconazole resistance mechanisms in *Candida albicans*. *Beilstein J Org Chem*. 2013;9(1):1501–1507. doi:10.3762/bjoc.9.171
8. Vandeputte P, Ferrari S, Coste AT. Antifungal resistance and new strategies to control fungal infections. *Int J Microbiol*. 2011;2012(3):1–26. doi:10.1155/2012/713687
9. Hancock RE, Sahl H-G. Antimicrobial and host-defense peptides as new anti-infective therapeutic strategies. *Nat Biotechnol*. 2006;24(12):1551. doi:10.1038/nbt1267
10. Zasloff M. Antimicrobial peptides of multicellular organisms. *nature*. 2002;415(6870):389. doi:10.1038/415389a
11. Galdiero E, Siciliano A, Maselli V, et al. An integrated study on antimicrobial activity and ecotoxicity of quantum dots and quantum dots coated with the antimicrobial peptide indolicidin. *Int J Nanomedicine*. 2016;11:4199. doi:10.2147/IJN.S107752
12. Maselli V, Siciliano A, Giorgio A, et al. Multigenerational effects and DNA alterations of QDs-indolicidin on daphnia magna. *Environ Pollut*. 2017;224:597–605. doi:10.1016/j.envpol.2017.02.043
13. Galdiero S, Falanga A, Berisio R, Grieco P, Morelli G, Galdiero M. Antimicrobial peptides as an opportunity against bacterial diseases. *Curr Med Chem*. 2015;22(14):1665–1677.
14. Abdul Ghaffar K, M Hussein W, G Khalil Z, J Capon R, Skwarczynski M, Toth I. Levofloxacin and indolicidin for combination antimicrobial therapy. *Curr Drug Deliv*. 2015;12(1):108–114.
15. Subbalakshmi C, Sitaram N. Mechanism of antimicrobial action of indolicidin. *FEMS Microbiol Lett*. 1998;160(1):91–96. doi:10.1111/j.1574-6968.1998.tb12896.x
16. Falla TJ, Karunaratne DN, Hancock RE. Mode of action of the antimicrobial peptide indolicidin. *J Biol Chem*. 1996;271(32):19298–19303. doi:10.1074/jbc.271.32.19298
17. Brogden NK, Brogden KA. Will new generations of modified antimicrobial peptides improve their potential as pharmaceuticals? *Int J Antimicrob Agents*. 2011;38(3):217–225. doi:10.1016/j.ijantimicag.2011.05.004
18. Kang S-J, Park SJ, Mishig-Ochir T, Lee B-J. Antimicrobial peptides: therapeutic potentials. *Expert Rev Anti-Infect Ther*. 2014;12(12):1477–1486. doi:10.1586/14787210.2014.976613
19. Azam A, Ahmed AS, Oves M, Khan MS, Habib SS, Memic A. Antimicrobial activity of metal oxide nanoparticles against Gram-positive and Gram-negative bacteria: a comparative study. *Int J Nanomedicine*. 2012;7:6003. doi:10.2147/IJN.S30631
20. Raghunath A, Perumal E. Metal oxide nanoparticles as antimicrobial agents: a promise for the future. *Int J Antimicrob Agents*. 2017;49(2):137–152. doi:10.1016/j.ijantimicag.2016.11.011
21. Torres L, Braga N, Gomes I, et al. Nanobiostructure of fibrous-like alumina functionalized with an analog of the BP100 peptide: synthesis, characterization and biological applications. *Colloids Surf B Biointerfaces*. 2018;163:275–283. doi:10.1016/j.colsurfb.2018.01.001
22. Brandelli A. Nanostructures as promising tools for delivery of antimicrobial peptides. *Mini Rev Med Chem*. 2012;12(8):731–741.
23. De Jong WH, Borm PJ. Drug delivery and nanoparticles: applications and hazards. *Int J Nanomedicine*. 2008;3(2):133. doi:10.2147/IJN.S596
24. Allahverdiyev AM, Kon KV, Abamor ES, Bagirova M, Rafailovich M. Coping with antibiotic resistance: combining nanoparticles with antibiotics and other antimicrobial agents. *Expert Rev Anti-Infect Ther*. 2011;9(11):1035–1052. doi:10.1586/eri.11.121
25. Zhao J, Zhao C, Liang G, Zhang M, Zheng J. Engineering antimicrobial peptides with improved antimicrobial and hemolytic activities. *J Chem Inf Model*. 2013;53(12):3280–3296. doi:10.1021/ci400477e
26. Yang X, Yang M, Pang B, Vara M, Xia Y. Gold nanomaterials at work in biomedicine. *Chem Rev*. 2015;115(19):10410–10488. doi:10.1021/acs.chemrev.5b00193
27. Connor EE, Mwamuka J, Gole A, Murphy CJ, Wyatt MD. Gold nanoparticles are taken up by human cells but do not cause acute cytotoxicity. *Small*. 2005;1(3):325–327. doi:10.1002/smll.200400093
28. de Alteriis E, Falanga A, Galdiero S, Guida M, Maselli V, Galdiero E. Genotoxicity of gold nanoparticles functionalized with indolicidin towards *Saccharomyces cerevisiae*. *J Environ Sci*. 2018;66:138–145. doi:10.1016/j.jes.2017.04.034
29. Huang W-C, Tsai P-J, Chen Y-C. Functional gold nanoparticles as photothermal agents for selective-killing of pathogenic bacteria. *Nanomedicine (Lond)*. 2007;2(6):777–787.
30. de Alteriis E, Maselli V, Falanga A, et al. Efficiency of gold nanoparticles coated with the antimicrobial peptide indolicidin against biofilm formation and development of *Candida* spp. clinical isolates. *Infect Drug Resist*. 2018;11:915. doi:10.2147/IDR.S164262
31. Jayaseelan C, Ramkumar R, Rahuman AA, Perumal P. Green synthesis of gold nanoparticles using seed aqueous extract of *Abelmoschus esculentus* and its antifungal activity. *Ind Crops Prod*. 2013;45:423–429. doi:10.1016/j.indcrop.2012.12.019
32. Wani IA, Ahmad T. Size and shape dependant antifungal activity of gold nanoparticles: a case study of *Candida*. *Colloids Surf B Biointerfaces*. 2013;101:162–170. doi:10.1016/j.colsurfb.2012.06.005
33. CLSI. *Reference Method for Broth Dilution Antifungal Susceptibility Testing of Yeasts; Approved Standard – Third Edition – Document M27-A3*. Wayne, PA: Clinical and Laboratory Standards Institute (CLSI); 2008.
34. CLSI C. *Reference Method for Broth Dilution Antifungal Susceptibility Testing of Yeasts: Fourth Informational Supplement M27-S4*. Wayne, PA: Clinical and Laboratory Standards Institute (CLSI); 2012.
35. Dechsakulthorn F, Hayes A, Bakand S, Joeng L, Winder C. In vitro cytotoxicity assessment of selected nanoparticles using human skin fibroblasts. *AATEX journal*. 2008;14(special issue):397–400.
36. Lee Y, Geckeler KE. Cytotoxicity and cellular uptake of lysozyme-stabilized gold nanoparticles. *J Biomed Mater Res A*. 2012;100(4):848–855. doi:10.1002/jbm.a.34020
37. Struck M, Gille J. Fungal infections in burns: a comprehensive review. *Ann Burns Fire Disasters*. 2013;26(3):147.
38. Ghosh P, Han G, De M, Kim CK, Rotello VM. Gold nanoparticles in delivery applications. *Adv Drug Deliv Rev*. 2008;60(11):1307–1315. doi:10.1016/j.addr.2008.03.016
39. Han G, Ghosh P, Rotello VM. Functionalized gold nanoparticles for drug delivery. *Nanomedicine (Lond)*. 2007;2(1):113–123. doi:10.1094/PDIS-91-4-0467B
40. Kimling J, Maier M, Okenve B, Kotaidis V, Ballot H, Plech A. Turkevich method for gold nanoparticle synthesis revisited. *J Phys Chem B*. 2006;110(32):15700–15707. doi:10.1021/jp061667w
41. Seol SK, Kim D, Jung S, Hwu Y. Microwave synthesis of gold nanoparticles: effect of applied microwave power and solution pH. *Mater Chem Phys*. 2011;131(1–2):331–335. doi:10.1016/j.matchemphys.2011.09.050
42. Sur A, Pradhan B, Banerjee A, Aich P. Immune activation efficacy of indolicidin is enhanced upon conjugation with carbon nanotubes and gold nanoparticles. *PLoS One*. 2015;10(4):e0123905. doi:10.1371/journal.pone.0123905
43. Delattin N, De Brucker K, De Cremer K, PA Cammue B, Thevissen K. Antimicrobial peptides as a strategy to combat fungal biofilms. *Curr Top Med Chem*. 2017;17(5):604–612.
44. Farzanegan A, Roudbary M, Falahati M, et al. Synthesis, characterization and antifungal activity of a novel formulated nanocomposite containing indolicidin and graphene oxide against disseminated candidiasis. *J Mycol Med*. 2018;28(4):628–636. doi:10.1016/j.mycmed.2018.07.009
45. Alvendal C, Ehrström S, Brauner A, Lundberg JO, Bohm-Starke N. Elevated nitric oxide in recurrent vulvovaginal candidiasis-association with clinical findings. *Acta Obst Gyn Scand*. 2017;96(3):295–301. doi:10.1111/aogs.13093

46. Vazquez-Torres A, Jones-Carson J, Warner T, Balish E. Nitric oxide enhances resistance of SCID mice to mucosal candidiasis. *J Infect Dis*. 1995;172(1):192–198. doi:10.1093/infdis/172.1.192
47. Elahi S, Pang G, Ashman RB, Clancy R. Nitric oxide-enhanced resistance to oral candidiasis. *Immunology*. 2001;104(4):447–454. doi:10.1046/j.1365-2567.2001.01331.x
48. Jones-Carson J, Vazquez-Torres A, van der Heyde HC, Warner T, Wagner RD, Balish E. γδ T cell-induced nitric oxide production enhances resistance to mucosal candidiasis. *Nat Med*. 1995;1(6):552.
49. Moncada S. Nitric oxide: physiology, pathophysiology, and pharmacology. *Pharmacol Rev*. 1991;43:109–142.
50. Archer S. Measurement of nitric oxide in biological models. *Faseb J*. 1993;7(2):349–360. doi:10.1096/fasebj.7.2.8440411
51. Knowles RG, Moncada S. Nitric oxide synthases in mammals. *Biochem J*. 1994;298(Pt 2):249. doi:10.1042/bj2980249

Supplementary materials

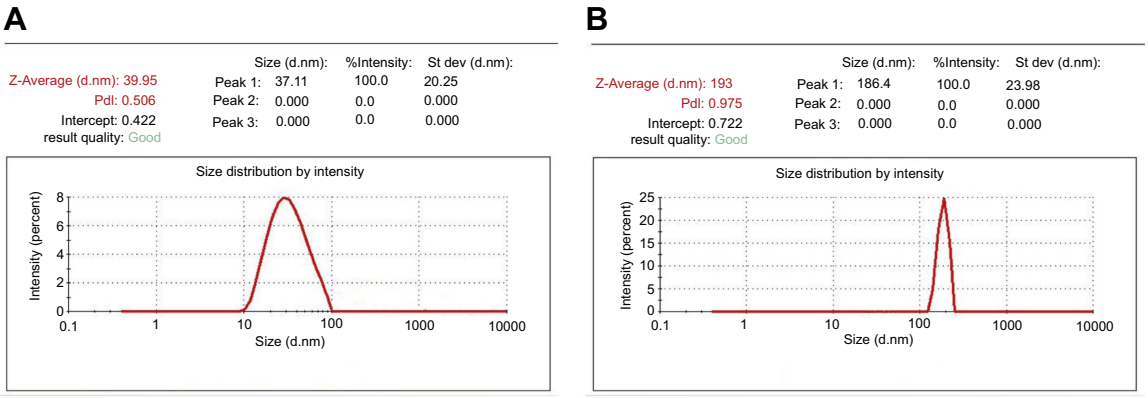

Figure S1 Size distribution by density of thiol-capped gold nanoparticles (NPs) and indolicidin-gold NPs conjugates is shown. The average size of thiol-capped gold nanoparticles was about 40 nm (**A**) and the average size of indolicidin conjugated with gold NPs was about 193 nm (**B**).

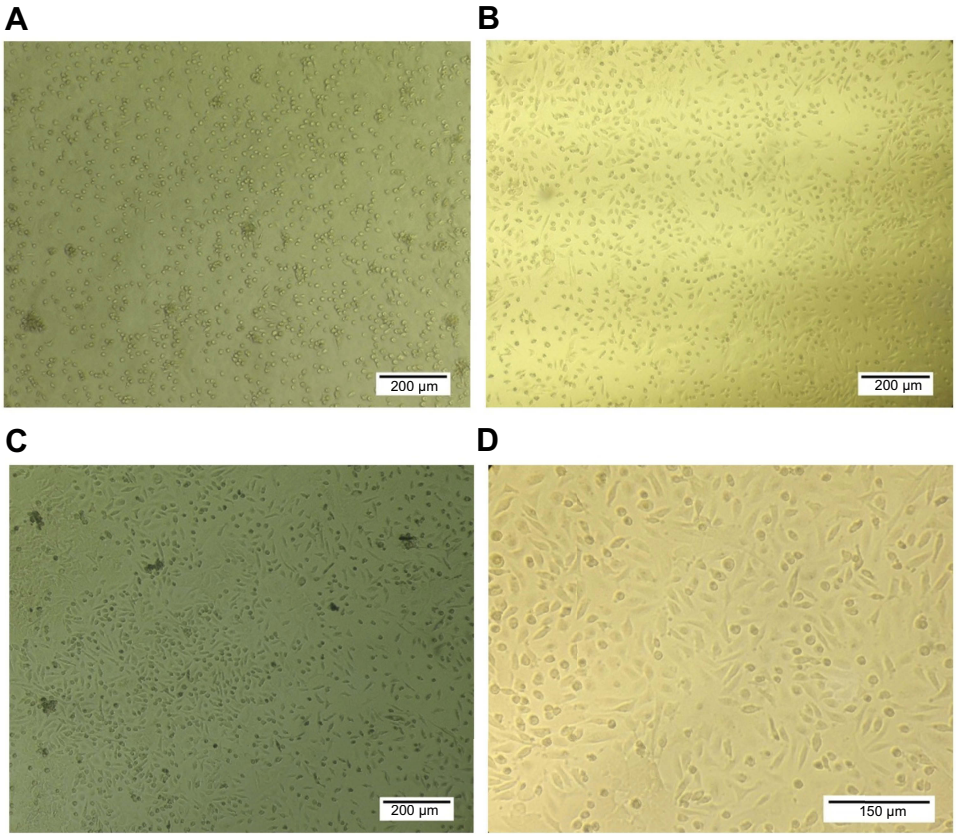

Figure S2 Morphological assessment of macrophages isolated from mice peritoneal cavity. Microscopy images of macrophages phenotype on day 2 (**A**), day 7 (**B**), and day 14 with 10× magnification (**C**), and day 14 with 20× magnification (**D**).